

Electronic Supplementary Information

Conjugated Ligand-based Tribochromic Luminescence

Angela M. Kuchison, Michael O. Wolf* and Brian O. Patrick

Department of Chemistry, University of British Columbia, Vancouver British Columbia,

*V6T 1Z1. *E-mail: mwolf@chem.ubc.ca*

Experimental Details

General. 3,3''-Dibromo-2,2':5',2''-terthiophene (Br_2T_3) and $\text{AuCl}(\text{tht})$ were synthesized according to literature procedures.^{1, 2} ^1H and $^{31}\text{P}\{^1\text{H}\}$ NMR spectroscopy experiments were carried out on a Bruker AV-300 spectrometer. The ^1H NMR spectra were referenced to residual solvent and the $^{31}\text{P}\{^1\text{H}\}$ NMR spectra were referenced to external 85% H_3PO_4 . Solution absorption spectra were recorded on a Cary 5000 UV/vis/near-IR spectrometer and the emission spectra were recorded on a Cary Eclipse spectrometer. Powder absorption spectra of $(\text{AuCl})_2\text{P}_2\text{T}_3$ were obtained using an Ocean Optics SD2000 fiber optics spectrometer with a DH-2000 mikropack UV-Vis-NIR light source. For these measurements, the $(\text{AuCl})_2\text{P}_2\text{T}_3$ was diluted with MgO (~1 mg of $(\text{AuCl})_2\text{P}_2\text{T}_3$ in 50 mg of MgO). Fluorescence lifetime measurements were carried out using a Horiba Jobin Yvon TBX Picosecond Photon Detection Module (Nanoled 370 nm) for P_2T_3 and a Princeton Instruments Spectra Pro 2300i Imaging Triple Grating Monochromator/Spectrograph with a Hamamatsu Dynamic Range Streak Camera (excitation source: EKSPLA Nd:YAG laser, $\lambda = 355$ nm) for $(\text{AuCl})_2\text{P}_2\text{T}_3$. Raman spectra were carried out using a Renishaw System 1000 confocal microscope with a 785 nm diode laser source and charge-coupled device (CCD) detector. Spectra were collected

for 30 s from 350-1800 cm^{-1} using 1% laser power. Powder XRD (PXRD) data were recorded on a Bruker D8 Advance diffractometer with graphite monochromated $\text{Cu K}\alpha$ radiation. The $(\text{AuCl})_2\text{P}_2\text{T}_3$ powder used for the PXRD was crushed after the measurement on a zero background silicon wafer and a diffractogram was then obtained.

Solid State Emission Spectroscopy

Samples of $(\text{AuCl})_2\text{P}_2\text{T}_3 \cdot \text{CH}_2\text{Cl}_2$ for emission measurements were recrystallized four times from $\text{CHCl}_3/\text{CH}_2\text{Cl}_2/\text{hexanes}$. To prepare thin films of $(\text{AuCl})_2\text{P}_2\text{T}_3$ for emission measurements, the solid was dissolved in minimal CHCl_3 and the solution drop-cast onto a quartz slide and dried at room temperature. The emission spectrum of $(\text{AuCl})_2\text{P}_2\text{T}_3$ was obtained by preparing a slurry of $(\text{AuCl})_2\text{P}_2\text{T}_3$ in hexanes which was drop-cast onto a quartz slide and dried at room temperature. The ground $(\text{AuCl})_2\text{P}_2\text{T}_3$ sample was prepared by pressing a second quartz slide on top of the slide of microcrystalline $(\text{AuCl})_2\text{P}_2\text{T}_3$ and then twisting the two slides while pressing them against each other.

X-Ray Crystallographic Analysis of $(\text{AuCl})_2\text{P}_2\text{T}_3$

A pale yellow plate-shaped crystal of $(\text{AuCl})_2\text{P}_2\text{T}_3$, having dimensions $0.30 \times 0.20 \times 0.015 \text{ mm}^3$, was placed on the tip of a mitegen micromount with paratone[®] oil. The sample was then cooled to 113(2) K using an Oxford Cryostream controller. Data was collected in the range $3^\circ \leq 2\theta \leq 63^\circ$ on a Bruker SMART diffractometer equipped with an APEX II CCD detector and a graphite monochromated $\text{Mo K}\alpha$ sealed X-ray tube operating at 1.5 kW (50 kV, 30 mA). The data were corrected by integration for the effects of absorption with a transmission range 0.490 – 0.746. Final unit-cell dimensions were determined on the basis of 9991 well-centred reflections with range $4^\circ \leq 2\theta \leq 63^\circ$.

The programs used for the absorption correction, and data reduction were from the Bruker APEX II Crystal Structure System. The structure was solved with Sir92 and refined using CRYSTALS.³ Diagrams were made using ORTEP-3,⁴ and POV-RAY.⁵ Complex scattering factors for neutral atoms were used in the calculation of structure factors.⁶

The structure appeared to exhibit some disorder due to rotation about two of the C-P bond. Due to the low (5%) disorder only the gold atoms were found, but are not included in our model. One of the dichloromethane units and a thiophene unit were also found to be disordered and were treated accordingly. Selected bond lengths and angles for one of the two molecules of $(\text{AuCl})_2\text{P}_2\text{T}_3$ can be found in Table S3.

X-Ray Crystallographic Analysis of P_2T_3

An orange plate crystal of $\text{C}_{36}\text{H}_{26}\text{P}_2\text{S}_3$ having approximate dimensions of $0.03 \times 0.18 \times 0.25$ mm was mounted on a glass fiber. Data were collected at a temperature of $-100.0 \pm 0.1^\circ\text{C}$ to a maximum 2θ value of 56.1° , on a Bruker X8 APEX II diffractometer with graphite monochromated Mo- $\text{K}\alpha$ radiation. Data were collected in a series of ϕ and ω scans in 0.50° oscillations with 20.0 second exposures. The crystal-to-detector distance was 36.00 mm.

Of the 24614 reflections that were collected, 7094 were unique ($R_{\text{int}} = 0.050$); equivalent reflections were merged. Data were collected and integrated using the Bruker SAINT⁷ software package. The linear absorption coefficient, μ , for Mo- $\text{K}\alpha$ radiation is 3.84 cm^{-1} . Data were corrected for absorption effects using the multi-scan technique (SADABS⁸), with minimum and maximum transmission coefficients of 0.884 and 0.989, respectively. The data were corrected for Lorentz and polarization effects.

The structure was solved by direct methods⁹. All non-hydrogen atoms were refined anisotropically. All hydrogen atoms were placed in calculated positions but were not refined. The final cycle of full-matrix least-squares refinement (Least Squares function minimized: $\sum w(F_o^2 - F_c^2)^2$) on F^2 was based on 7094 reflections and 370 variable parameters and converged (largest parameter shift was 0.00 times its esd) with unweighted and weighted agreement factors of:

$$R1 = \sum ||F_o| - |F_c|| / \sum |F_o| = 0.095$$

$$wR2 = [\sum (w (F_o^2 - F_c^2)^2) / \sum w(F_o^2)^2]^{1/2} = 0.108$$

The standard deviation of an observation of unit weight (Standard deviation of an observation of unit weight: $[\sum w(F_o^2 - F_c^2)^2 / (N_o - N_v)]^{1/2}$; where: N_o = number of observations, N_v = number of variables) was 1.00. The weighting scheme was based on counting statistics. The maximum and minimum peaks on the final difference Fourier map corresponded to 0.51 and $-0.32 \text{ e}^-/\text{\AA}^3$, respectively.

Neutral atom scattering factors were taken from Cromer and Waber.¹⁰ Anomalous dispersion effects were included in F_{calc} ;¹¹ the values for $\Delta f'$ and $\Delta f''$ were those of Creagh and McAuley¹². The values for the mass attenuation coefficients are those of Creagh and Hubbell¹³. All refinements were performed using the SHELXTL¹⁴ crystallographic software package of Bruker-AXS. Diagrams were made using ORTEP-3,⁴ and POV-RAY.⁵

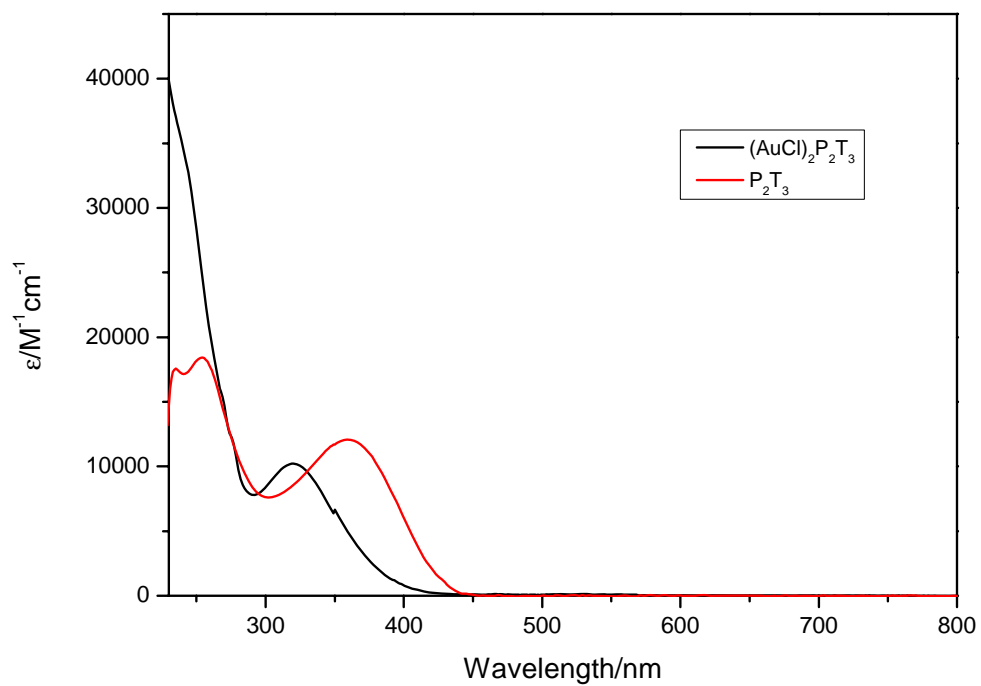


Figure S1. Absorption spectra of $(\text{AuCl})_2\text{P}_2\text{T}_3$ and P_2T_3 in CH_2Cl_2 .

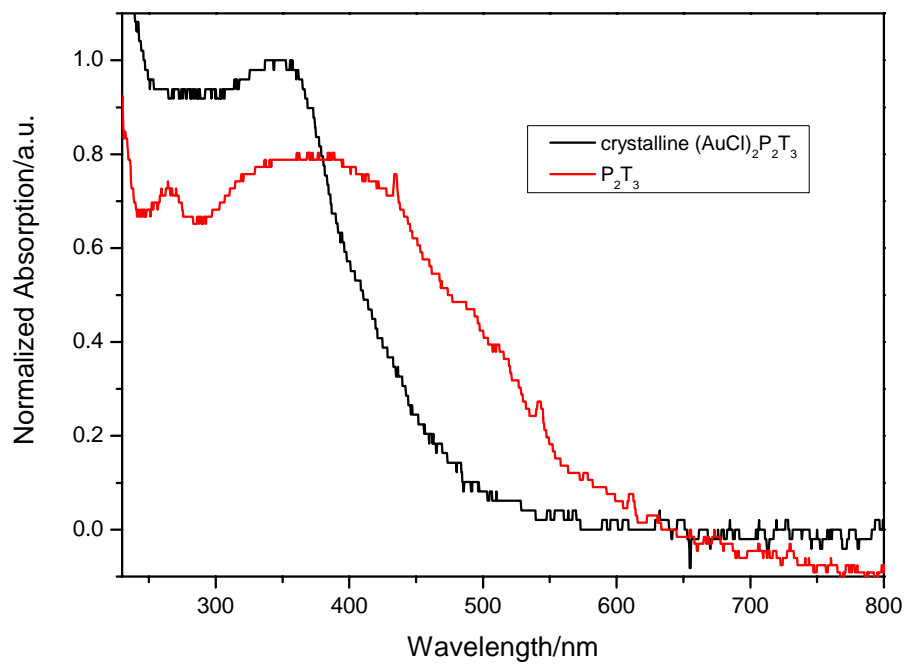


Figure S2. Solid state absorption spectra of $(\text{AuCl})_2\text{P}_2\text{T}_3$ and P_2T_3 .

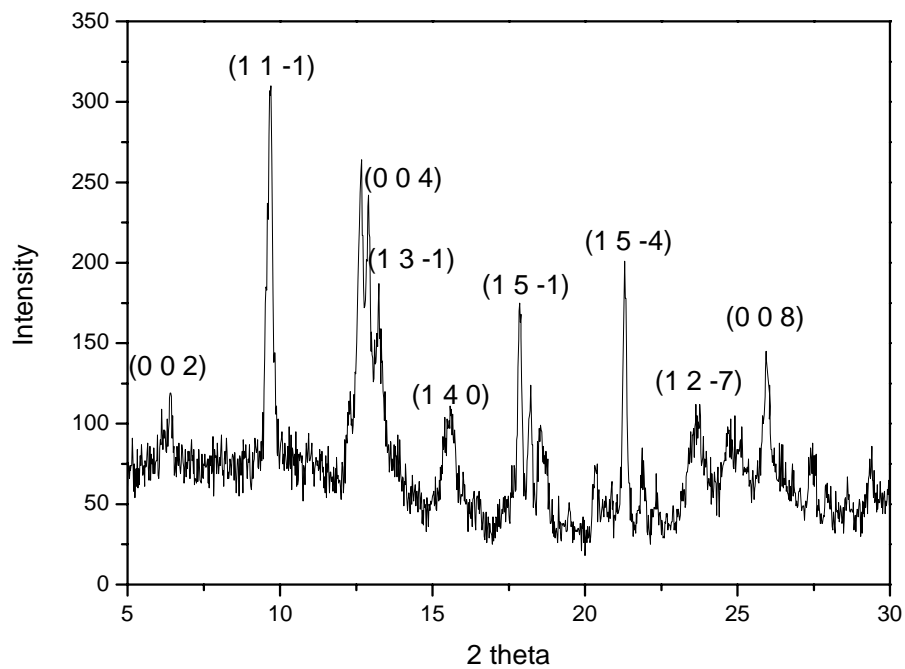


Figure S3. Powder XRD of microcrystalline $(\text{AuCl})_2\text{P}_2\text{T}_3$.

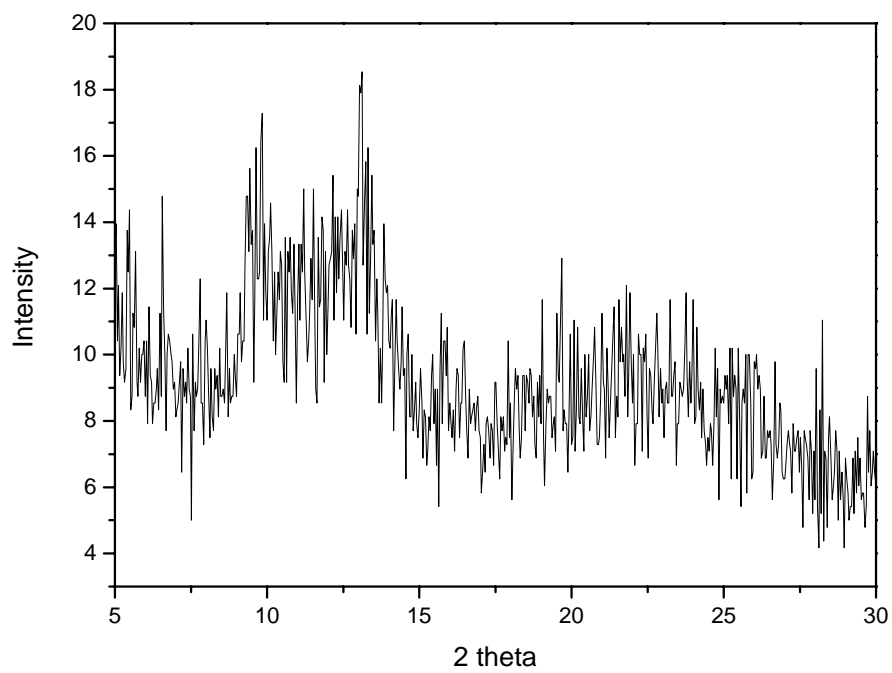


Figure S4. Powder XRD of ground $(\text{AuCl})_2\text{P}_2\text{T}_3$.

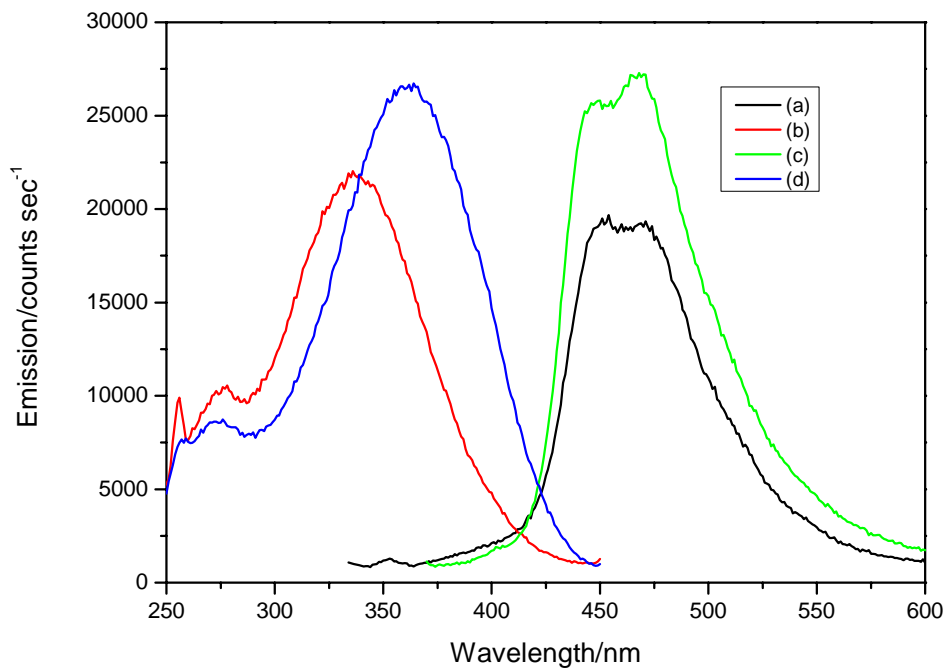


Figure S5. Emission and excitation spectra of $(\text{AuCl})_2\text{P}_2\text{T}_3$ and P_2T_3 in CH_2Cl_2 (a) emission scan of $(\text{AuCl})_2\text{P}_2\text{T}_3$, $\lambda_{\text{ex}} = 320$ nm; (b) excitation scan of $(\text{AuCl})_2\text{P}_2\text{T}_3$, $\lambda_{\text{em}} = 460$ nm; (c) emission scan of P_2T_3 , $\lambda_{\text{ex}} = 360$ nm; (d), excitation scan of P_2T_3 , $\lambda_{\text{em}} = 460$ nm.

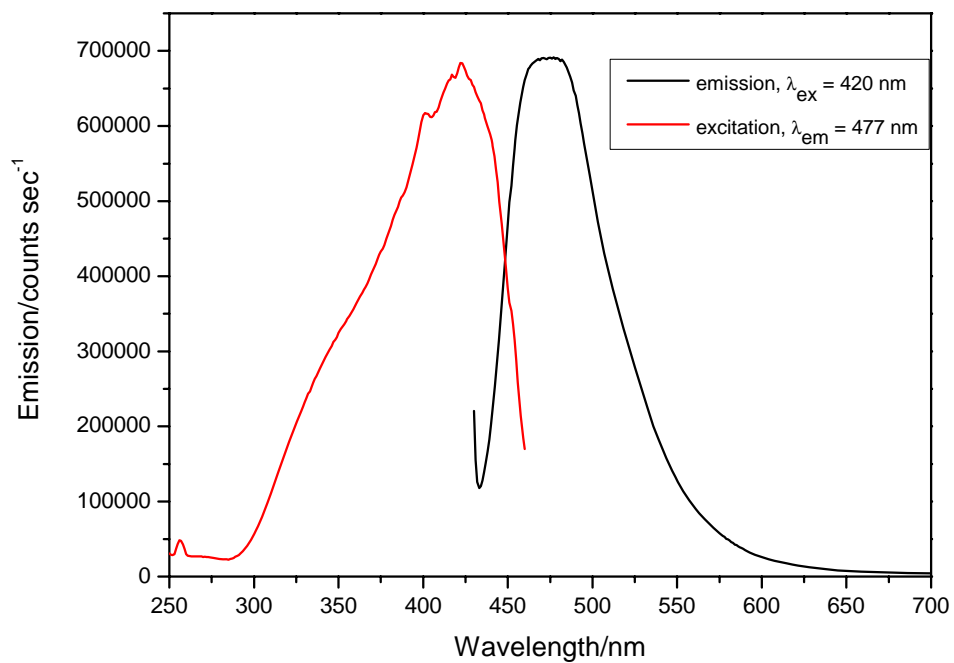


Figure S6. Excitation and emission spectra of solid, ground (AuCl)₂P₂T₃.

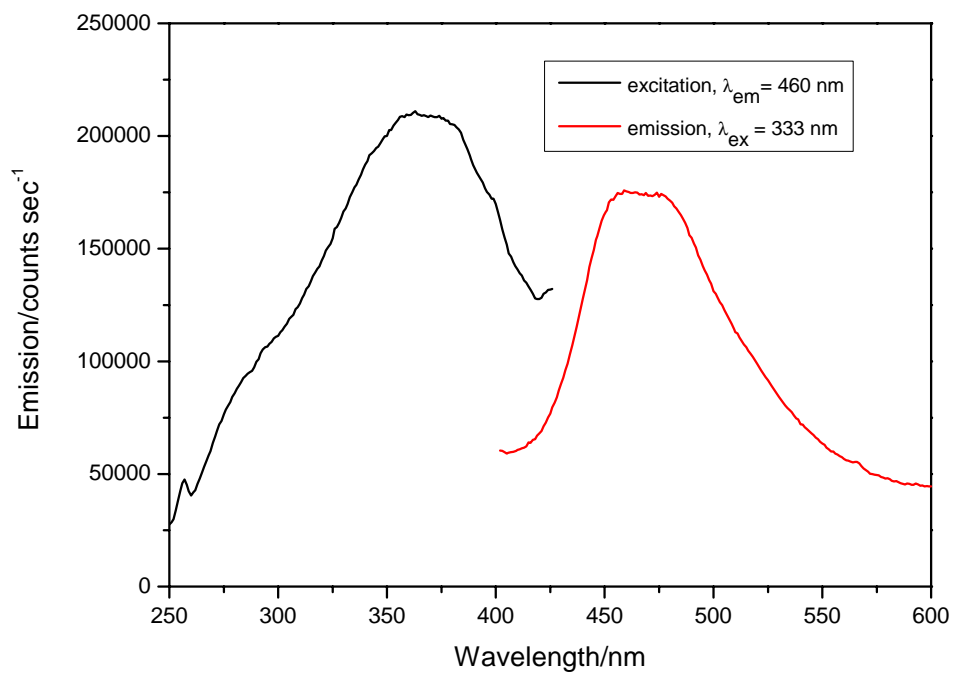


Figure S7. Excitation and emission spectra of (AuCl)₂P₂T₃ (dropcast film).

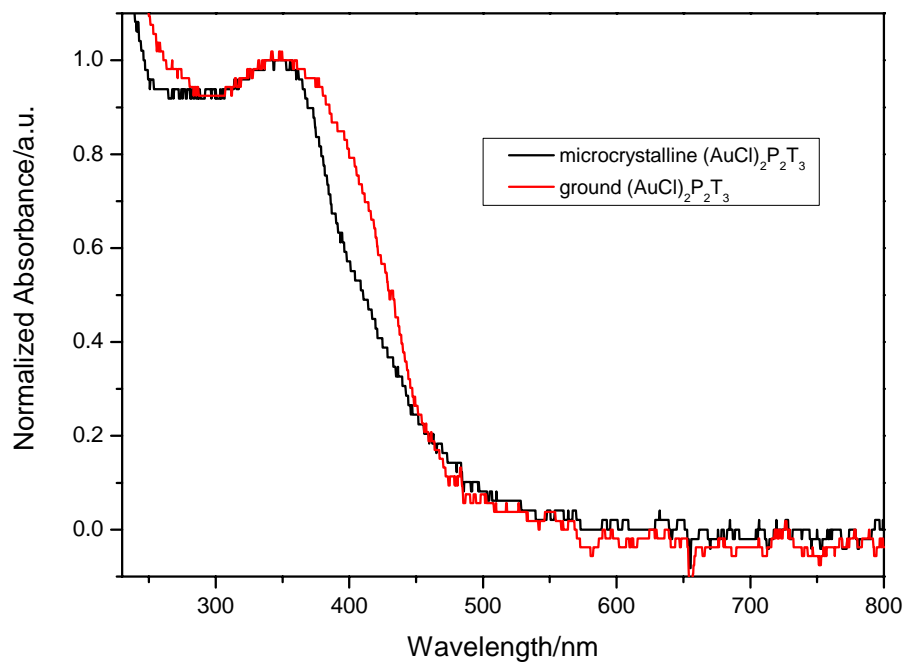


Figure S8. Absorption spectra of (AuCl)₂P₂T₃.

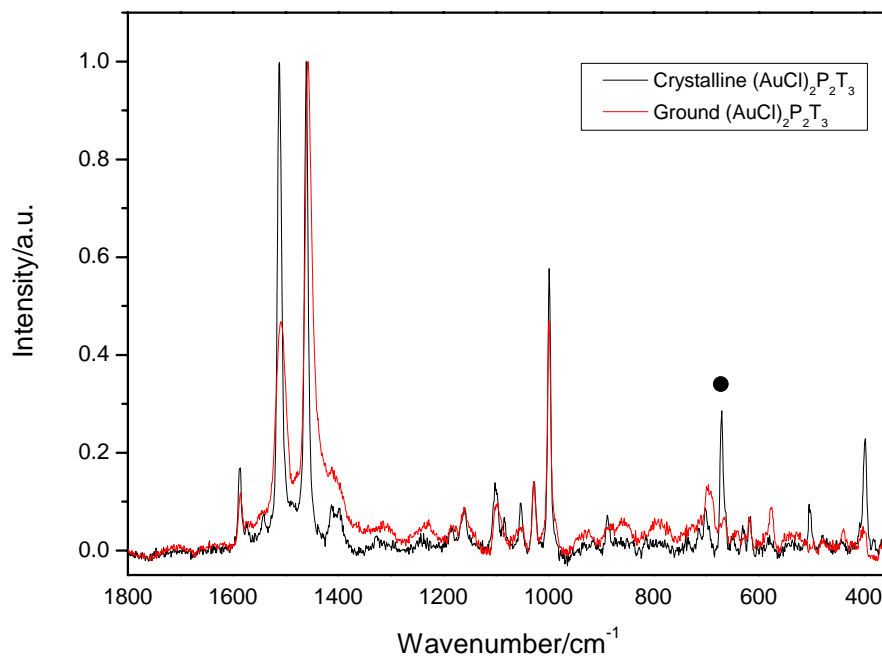


Figure S9. Baseline corrected Raman spectra of crystals of $(\text{AuCl})_2\text{P}_2\text{T}_3$ and ground crystals of $(\text{AuCl})_2\text{P}_2\text{T}_3$.

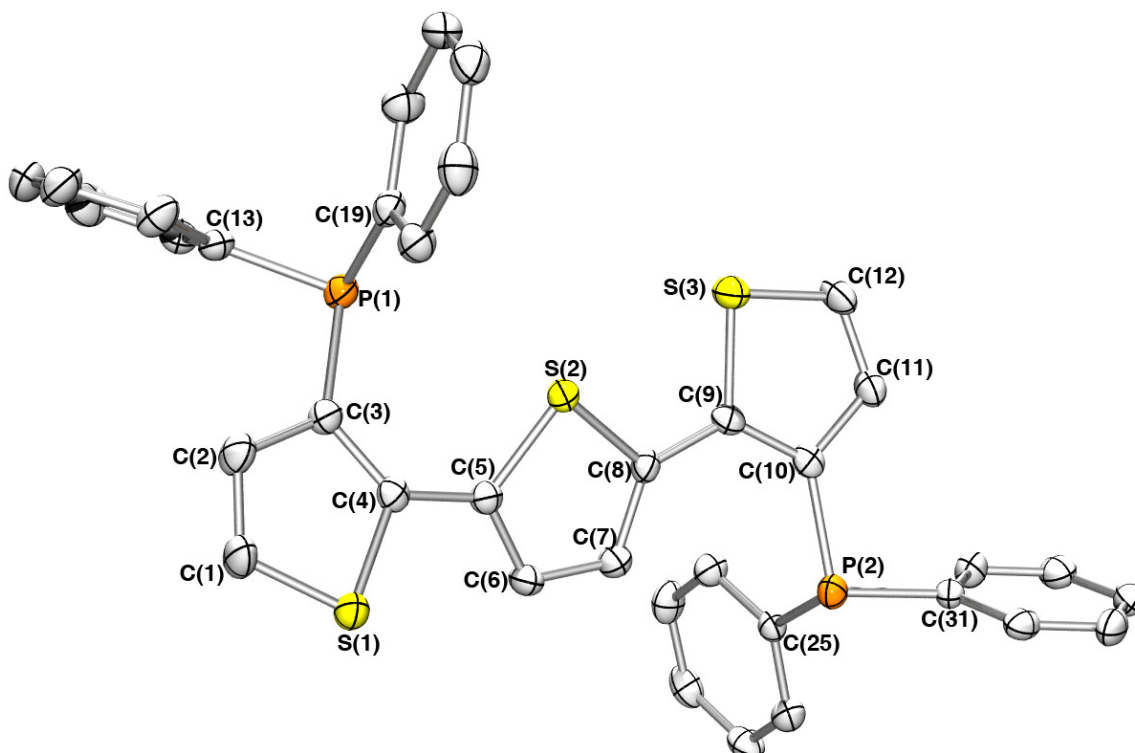


Figure S11. Solid-state molecular structure of P₂T₃. Hydrogen atoms are omitted for clarity and thermal ellipsoids are drawn at 50% probability.

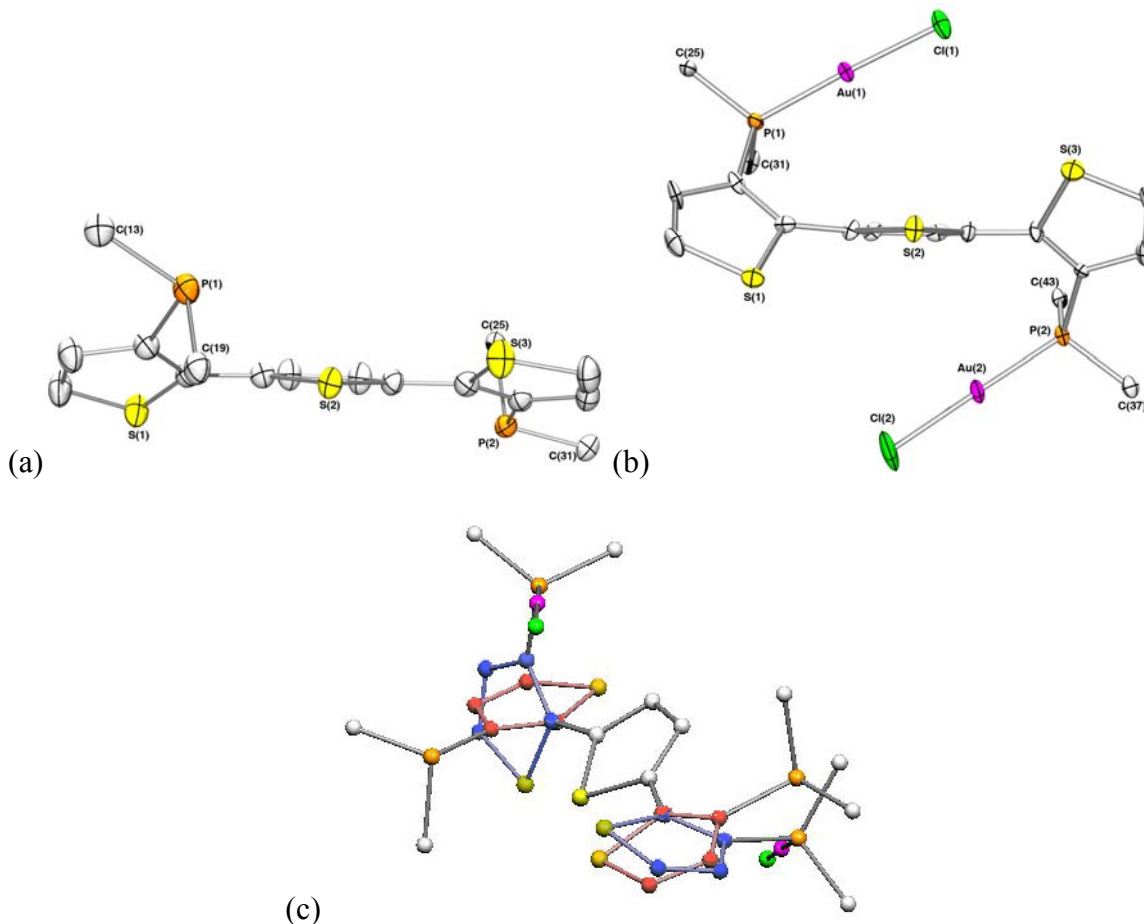


Figure S12. Solid-state molecular structures of (a) P₂T₃, (b) Molecule A of (AuCl)₂P₂T₃ showing the interannular torsion angle differences. Hydrogen atoms, occluded, and phenyl rings are omitted for clarity and thermal ellipsoids are drawn at 50% probability. (c) superimposed image of the atomic coordinates of P₂T₃ (with terminal thiophenes highlighted in red) and (AuCl)₂P₂T₃ (with terminal thiophenes highlighted in blue) generated from their solid-state molecular structures with phenyl rings and hydrogen atoms omitted for clarity.

Table S1. Assignments of Raman bands for crystalline $(\text{AuCl})_2\text{P}_2\text{T}_3$ and ground $(\text{AuCl})_2\text{P}_2\text{T}_3$.

Crystalline $(\text{AuCl})_2\text{P}_2\text{T}_3$		Ground $(\text{AuCl})_2\text{P}_2\text{T}_3$	
Band (cm^{-1})	Assignment	Band (cm^{-1})	Assignment
1586 (w)	$\nu(\text{C}=\text{C})$ (ph)*	1586 (w)	$\nu(\text{C}=\text{C})$ (ph)*
1512 (s)	$\nu_{\text{asym}}(\text{C}=\text{C})$ (th)**	1509 (s)	$\nu_{\text{asym}}(\text{C}=\text{C})$ (th)**
1460 (s)	$\nu_{\text{sym}}(\text{C}=\text{C})$ (th)**	1457 (s)	$\nu_{\text{sym}}(\text{C}=\text{C})$ (th)**
1400 (br, w)	$\nu(\text{C}-\text{C})$ (th)**	1400 (br, vw)	$\nu(\text{C}-\text{C})$ (th)**
1158(w), 1101(w), 1053(w), 1028(w)	$\delta(\text{C}-\text{H})$ ** and $\nu(\text{P}-\text{C})$ *	1157(w), 1100(w), 1056(w), 1028 (w)	$\delta(\text{C}-\text{H})$ ** and $\nu(\text{P}-\text{C})$ *
998 (s)	$\nu(\text{C}-\text{S})$ ** and/or ring breathing $\nu(\text{C}=\text{C})$ (ph)**	998 (s)	$\nu(\text{C}-\text{S})$ ** and/or ring breathing $\nu(\text{C}=\text{C})$ (ph)**
702 (w)	Ph vib*	695 (w)	Ph vib*
671 (m)	Ring bending (th)***	668 (vw)	Ring bending (th)***
504 (w)	Ring deformation*	616 (w)	Ring vibrations*
		577 (w)	Ring vibrations*

*Assignments based on reference.¹⁵

**Assignments based on reference.¹⁶

***Assignments based on reference.¹⁷

ph = phenyl, th = thienyl

Table S2. Selected Crystallographic Data for $(\text{AuCl})_2\text{P}_2\text{T}_3 \cdot \text{CH}_2\text{Cl}_2$ and P_2T_3 .

	$(\text{AuCl})_2\text{P}_2\text{T}_3 \cdot \text{CH}_2\text{Cl}_2$	P_2T_3
formula	$\text{C}_{37} \text{H}_{28} \text{Au}_2 \text{Cl}_4 \text{P}_2 \text{S}_3$	$\text{C}_{36}\text{H}_{26}\text{P}_2\text{S}_3$
habit	plate	plate
dimensions/mm	$0.015 \times 0.20 \times 0.30$	$0.03 \times 0.18 \times 0.25$
temperature/K	113(2)	173(2)
cryst syst	monoclinic	triclinic
space group	$\text{P } 2_1/c$ (#14)	$\text{P } \bar{1}$ (#2)
$a/\text{\AA}$	9.6976(2)	9.3829(7)
$b/\text{\AA}$	28.8439(6)	11.5838(9)
$c/\text{\AA}$	27.6767(6)	14.4954(12)
α/deg	90	89.673(4)
β/deg	97.3710(10)	72.855(4)
γ/deg	90	80.512(4)
$V/\text{\AA}^3$	7677.7(3)	1483.4(2)
Z	8	2
$\rho_{\text{calc}}/\text{g cm}^{-3}$	2.018	1.381
μ (Mo $\text{K}\alpha$)/ mm^{-1}	8.187	0.384
R^a ($I > 2.0\sigma(I)$)	0.0715	0.0462
R_w^a ($I > 2.0\sigma(I)$)	0.0669	0.0920
goodness of fit	1.15	1.00

^aFunction minimized $\sum w(|F_o| - |F_c|)^2$ $R = \sum ||F_o| - |F_c|| / \sum |F_o|$, $R_w = [\sum w(|F_o| - |F_c|)^2 / \sum w|F_o|^2]^{1/2}$.

Table S3. Selected bond lengths and angles of $(\text{AuCl})_2\text{P}_2\text{T}_3 \cdot \text{CH}_2\text{Cl}_2$.

(AuCl)₂P₂T₃ (A)		(AuCl)₂P₂T₃ (B)	
Bond Lengths (Å)			
Au(1)-Cl(1)	2.288(3)	Au(3)-Cl(3)	2.289(3)
Au(2)-Cl(2)	2.283(3)	Au(4)-Cl(4)	2.287(3)
Au(1)-P(1)	2.232(3)	Au(3)-P(3)	2.220(3)
Au(2)-P(2)	2.223(3)	Au(4)-P(4)	2.229(3)
P(1)-C(3)	1.791(11)	P(3)-C(15)	1.800(11)
P(1)-C(25)	1.807(12)	P(3)-C(49)	1.801(11)
P(1)-C(31)	1.812(12)	P(3)-C(55)	1.814(11)
P(2)-C(10)	1.804(10)	P(4)-C(22)	1.795(12)
P(2)-C(37)	1.815(12)	P(4)-C(61)	1.797(12)
P(2)-C(43)	1.811(11)	P(4)-C(67)	1.808(11)
S(1)-C(1)	1.723(14)	S(6)-C(21)	1.719(11)
S(1)-C(4)	1.736(11)	S(6)-C(24)	1.703(15)
C(1)-C(2)	1.335(17)	C(21)-C(22)	1.378(15)
C(2)-C(3)	1.426(15)	C(22)-C(23)	1.443(16)
C(3)-C(4)	1.414(16)	C(23)-C(24)	1.367(17)
C(4)-C(5)	1.440(15)	C(20)-C(21)	1.494(12)
Angles (deg)			
Cl(1)-Au(1)-P(1)	177.14(11)	Cl(3)-Au(3)-P(3)	177.22(13)
Cl(2)-Au(2)-P(2)	178.47(17)	Cl(4)-Au(4)-P(4)	178.85(12)

Au(1)-P(1)-C(3)	112.1(3)	Au(4)-P(4)-C(22)	111.3(4)
Au(1)-P(1)-C(25)	115.6(4)	Au(4)-P(4)-C(61)	114.9(4)
C(3)-P(1)-C(25)	101.9(5)	C(22)-P(4)-C(61)	104.4(5)
Au(1)-P(1)-C(31)	114.5(4)	Au(4)-P(4)-C(67)	114.1(4)
C(3)-P(1)-C(31)	106.6(5)	C(22)-P(4)-C(67)	106.2(5)
C(25)-P(1)-C(31)	105.0(5)	C(61)-P(4)-C(67)	105.0(5)
C(1)-S(1)-C(4)	92.4(6)	C(21)-S(6)-C(24)	91.5(6)
S(1)-C(1)-C(2)	111.2(9)	C(23)-C(24)-S(6)	112.5(9)
C(1)-C(2)-C(3)	115.6(11)	C(22)-C(23)-C(24)	112.7(11)
C(2)-C(3)-C(4)	110.3(10)	C(21)-C(22)-C(23)	110.4(10)
C(3)-C(4)-S(1)	110.5(8)	S(6)-C(21)-C(22)	112.8(8)
C(2)-C(3)-P(1)	127.7(9)	P(4)-C(22)-C(23)	125.5(9)
P(1)-C(3)-C(4)	121.7(8)	P(4)-C(22)-C(21)	123.7(8)
Torsion Angles (deg)			
S(1)-C(4)-C(5)-S(2)	51(1)	S(4)-C(16)-C(17)-S(5)	51(1)
S(2)-C(8)-C(9)-S(3)	-49(1)	S(5)-C(20)-C(21)-S(6)	50.3(9)

Table S5. Selected bond lengths and angles of P₂T₃.

Bond Lengths (Å)			
C(3)-P(1)	1.830(2)	C(19)-P(1)	1.834(2)
C(13)-P(1)	1.845(2)	C(10)-P(2)	1.826(3)
C(25)-P(2)	1.842(2)	C(31)-P(2)	1.833(2)
C(1)-C(2)	1.343(4)	C(1)-S(1)	1.707(3)
C(2)-C(3)	1.429(3)	C(3)-C(4)	1.376(3)
C(4)-C(5)	1.453(3)		
Angles (deg)			
C(3)-P(1)-C(19)	103.19(11)	C(3)-P(1)-C(13)	101.58(11)
C(19)-P(1)-C(13)	100.07(11)	C(2)-C(1)-S(1)	112.0(2)
C(1)-C(2)-C(3)	114.2(2)	C(4)-C(3)-C(2)	110.7(2)
C(4)-C(3)-P(1)	123.02(18)	C(2)-C(3)-P(1)	125.90(19)
C(3)-C(4)-S(1)	111.58(18)		
Torsion Angles (deg)			
S(1)-C(4)-C(5)-S(2)	-149.65(15)	S(2)-C(8)-C(9)-S(3)	-17.7(3)

References

1. A. Facchetti, M.-H. Yoon, C. L. Stern, G. R. Hutchison, M. A. Ratner, and T. J. Marks, *J. Am. Chem. Soc.*, 2004, **126**, 13480-13501.
2. R. Uson, A. Laguna, and J. Vicente, *J. Organomet. Chem.*, 1977, **131**, 471-475.
3. P. W. Betteridge, J. R. Carruthers, R. I. Cooper, K. Prout, and D. J. Watkin, *J. Appl. Crystallogr.*, 2003, **36**, 1487.
4. L. J. Farrugia, *J. Appl. Crystallogr.*, 1997, **30**, 565.
5. T. D. Fenn, D. Ringe, and G. A. Petsko, *J. Appl. Crystallogr.*, 2003, **36**, 944-947.
6. 'International Tables for X-ray Crystallography', IV, Kynoch Press: Birmingham, U.K. (present distributor Kluwer Academic Publishers: Boston, MA), 99, 1975.
7. SAINT. Version 7.03A. Bruker AXS Inc., Madison, Wisconsin, USA. 1997-2003.
8. SADABS. Bruker Nonius area detector scaling and absorption correction - V2.10. Bruker AXS Inc., Madison, Wisconsin, USA. 2003.
9. A. Altomare, M. C. Burla, M. Camalli, G. L. Casciarano, C. Giacovazzo, A. Guagliardi, A. G. G. Moliterni, G. Polidori, and R. Spagna, *J. Appl. Crystallogr.*, 1999, **32**, 115-119.
10. D. T. Cromer and J. T. Waber, 'International Tables for X-ray Crystallography', Vol. IV, The Kynoch Press, Birmingham, England, Table 2.2A, 1974.
11. J. A. Ibers and W. C. Hamilton, *Acta Cryst.*, 1964, **17**, 781-782.
12. D. C. Creagh and W. J. McAuley, 'International Tables for Crystallography', Vol C, (A.J.C. Wilson, ed.), Kluwer Academic Publishers, Boston, Table 4.2.6.8, pages 219-222, 1992.
13. D. C. Creagh and J. H. Hubbell, 'International Tables for Crystallography', Vol C, (A.J.C. Wilson, ed.), Kluwer Academic Publishers, Boston, Table 4.2.4.3, pages 200-206, 1992.
14. SHELXTL. Version 5.1. Bruker AXS Inc., Madison, Wisconsin, USA. 1997.
15. R. Faggiani, H. E. Howard-Lock, C. J. L. Lock, and M. A. Turner, *Can. J. Chem.*, 1987, **65**, 1568-1575.
16. F. Svedberg, Y. Alaverdyan, P. Johansson, and M. Käll, *J. Phys. Chem. B*, 2006, **110**, 25671-25677.
17. M. Akimoto, Y. Furukawa, H. Takeuchi, I. Harada, Y. Soma, and M. Soma, *Synth. Met.*, 1986, **15**, 353-360.